

Electrical resistivity and magnetoresistance of single-crystal $\text{Tb}_5\text{Si}_{2.2}\text{Ge}_{1.8}$ M. Zou,^{1,*} V. K. Pecharsky,^{1,2} K. A. Gschneidner, Jr.,^{1,2} Ya. Mudryk,¹ D. L. Schlager,¹ and T. A. Lograsso¹¹The Ames Laboratory, U.S. Department of Energy, Iowa State University, Ames, Iowa 50011-3020, USA²Department of Materials Science and Engineering, Iowa State University, Ames, Iowa 50011-2300, USA

(Received 24 August 2009; revised manuscript received 22 October 2009; published 16 November 2009)

A positive colossal magnetoresistance (CMR) of 160% has been observed in $\text{Tb}_5\text{Si}_{2.2}\text{Ge}_{1.8}$ with the magnetic field applied parallel to the a axis. When the magnetic field is applied parallel to the b and c axes, the magnetoresistance (MR) is less than 8% and 5%, respectively. The CMR effect originates from intrinsic crystallographic phase coexistence. The anisotropy of the MR effect is due to a unique geometric arrangement of the interphase boundaries and large magnetocrystalline anisotropy of the compound.

DOI: [10.1103/PhysRevB.80.174411](https://doi.org/10.1103/PhysRevB.80.174411)

PACS number(s): 72.15.-v, 75.47.Gk, 75.50.Cc

I. INTRODUCTION

Studies of electrical resistivities of metals and alloys have been an important part of condensed-matter physics because of their contributions to basic understanding of the electronic nature of materials and technological applications. The giant magnetoresistance (GMR) and colossal magnetoresistance (CMR) have been especially active fields over the last two decades.¹⁻⁶ In the past ten years, the GMR effect has been reported in the intermetallic compounds $R_5(\text{Si}_x\text{Ge}_{1-x})_4$, where R is a rare-earth metal, also known for their giant magnetocaloric effect.⁷⁻¹² Depending on the composition of the compound, the values of the GMR in this family of materials vary between 10% and 50%, which are comparable to those of the artificially fabricated GMR multilayers. Different from a spin-dependent scattering mechanism in the GMR multilayers, the GMR effects of $R_5(\text{Si}_x\text{Ge}_{1-x})_4$ compounds are associated with a coupled magnetic and crystallographic phase transformation which can be triggered by varying temperature, magnetic field, and/or pressure.¹³ Thus, the giant magnetoresistance of $R_5(\text{Si}_x\text{Ge}_{1-x})_4$ is similar in origin to the CMR effect in the perovskite manganites. Unlike the always negative magnetoresistance of the GMR multilayers and CMR manganites, the GMR in $R_5(\text{Si}_x\text{Ge}_{1-x})_4$ compounds can be either positive or negative, depending on composition.

The electrical resistivity as a function of temperature and magnetic field of one series of the $R_5(\text{Si}_x\text{Ge}_{1-x})_4$ family, $\text{Tb}_5(\text{Si}_x\text{Ge}_{1-x})_4$, has been studied for the compositions with $x=0.5, 0.6, 0.75$, and 1 using polycrystalline samples by different research groups.¹⁴⁻¹⁷ No abrupt change in the electrical resistivities was observed between 10 and 300 K for $\text{Tb}_5\text{Si}_3\text{Ge}$ and Tb_5Si_4 , in agreement with the crystallographic study of these compounds showing no crystallographic phase transformation in this temperature range.¹⁴ Polycrystalline $\text{Tb}_5\text{Si}_2\text{Ge}_2$ exhibited an abrupt 30% increase in the electrical resistivity at the crystallographic phase-transformation temperature upon heating and a negative magnetoresistance,¹⁵ similar to those observed in $\text{Gd}_5(\text{Si}_x\text{Ge}_{1-x})_4$ with $x=0.1, 0.45$, and 0.5 (Refs. 7-9). The magnetoresistance of the $\text{Tb}_5\text{Si}_2\text{Ge}_2$ compound, however, did not show a metamagnetic transition as observed in the counterpart Gd compound. The magnitude of the magnetoresistance in the former was substantially smaller than that in the latter. These differences were explained by an approximately 10 K decoupling of the

magnetic and crystallographic phase transformations in the $\text{Tb}_5\text{Si}_2\text{Ge}_2$ compound, leading to an incomplete magnetic field induced magnetic phase transition.¹⁵ Interestingly, a polycrystalline sample of $\text{Tb}_5\text{Si}_{2.4}\text{Ge}_{1.6}$ ($x=0.6$) showed a distinctly different electrical resistivity behavior at its crystallographic phase transformation characterized by an abrupt 40% drop of the electrical resistivity upon heating.¹⁷ Thus, this compound appears to have high resistivity rather than low resistivity at low temperatures—peculiarity also observed in other $R_5(\text{Si}_x\text{Ge}_{1-x})_4$ compounds.^{11,12}

Polycrystalline $\text{Tb}_5\text{Si}_{2.2}\text{Ge}_{1.8}$ ($x=0.55$) exhibits an incomplete crystallographic phase transition in the vicinity of its Curie temperature (T_C),¹⁸ similar to that observed in polycrystalline $\text{Tb}_5\text{Si}_2\text{Ge}_2$. An *in situ* x-ray powder-diffraction study of $\text{Tb}_5\text{Si}_{2.2}\text{Ge}_{1.8}$ near and above T_C showed that a 40 kOe external magnetic field can drive an approximately 30 mol % increase in the concentration of the orthorhombic phase, i.e., the magnetic field induces an incomplete crystallographic phase transition from the monoclinic to the orthorhombic structure. The magnetic field induced magnetic phase transitions, however, are complete when the external field is applied along the easy magnetization direction— a axis of a $\text{Tb}_5\text{Si}_{2.2}\text{Ge}_{1.8}$ single crystal. The x-ray powder-diffraction study of the $\text{Tb}_5\text{Si}_{2.2}\text{Ge}_{1.8}$ compound also showed that the temperature-induced crystallographic phase transformation between the high-temperature monoclinic and low-temperature orthorhombic phases is also incomplete. Upon cooling, about 20 vol % of the monoclinic phase is retained down to 5 K.¹⁸ This crystallographic phase coexistence, observed in the $\text{Dy}_5\text{Si}_3\text{Ge}$ compound as well,¹⁹ appears to be intrinsic to the $R_5(\text{Si}_x\text{Ge}_{1-x})_4$ family due to a competition among different magnetic and crystallographic thermodynamic energy scales. That is, the magnetic exchange energy favors the orthorhombic crystal structure at low temperatures, but the thermal energy, favors the low-temperature monoclinic state. Moreover, this competition is also at the foundation of the observed Griffiths phase-like behavior observed in $\text{Tb}_5\text{Si}_2\text{Ge}_2$ and $\text{Tb}_5\text{Si}_{2.2}\text{Ge}_{1.8}$.^{20,21}

It has been established that phase coexistence plays a key role in the CMR effects observed in some perovskite manganites. Theoretical studies have suggested that (i) the CMR effect is a Griffiths singularity²² and (ii) colossal magnetoresistance effects should be accompanied by the competition of ordered phases.²³ Considering this scenario, a further study of the phase coexistence and magnetoresistance in the

$R_5(\text{Si}_x\text{Ge}_{1-x})_4$ compounds is imperative. Here, we report an electrical resistivity study of high-purity $\text{Tb}_5\text{Si}_{2.2}\text{Ge}_{1.8}$ single crystals as a function of temperature, magnetic field, and crystallographic directions.

II. EXPERIMENTAL DETAILS

Two $\text{Tb}_5\text{Si}_{2.2}\text{Ge}_{1.8}$ single crystals were grown by the tri-arc method²⁴ from two stocks of high-purity Tb [99.67 at % (99.97 wt %) and 99.89 at % (99.99 wt %), respectively] prepared by the Materials Preparation Center of the Ames Laboratory,²⁵ and five nines pure (both) Si and Ge that were purchased from Atlantic Equipment Engineers of Micron Metals, Inc. and CERAC Inc., respectively. The as-grown crystals were oriented by using back-reflection Laue x-ray diffraction. Three samples for the electrical resistivity measurements were cut by spark erosion. The samples were parallelepipeds with dimensions of $5.03 \times 0.98 \times 0.44$, $3.38 \times 0.94 \times 0.57$, and $4.66 \times 1.02 \times 0.82$ mm³ with the longest dimensions along the *a*-, *b*-, and *c*-axes directions, respectively. The *a*- and *b*-axes samples came from the single crystal prepared using 99.67 at % pure Tb metal, and the *c*-axis sample from the 99.89 at % pure Tb.

The electrical resistances were measured using a standard four-probe method. Four thin platinum wires were attached to the samples with H20E Epotek silver epoxy manufactured by Epoxy Technology. The distances between the voltage contacts were 1.20, 1.14, and 3.03 mm for the *a*-, *b*-, and *c*-axes samples, respectively. Typical contact resistances were between 1 and 2 Ω . The temperature (*T*) and magnetic field (*H*) dependencies of the dc electrical resistance (*R*) were measured with a constant dc excitation electrical current (*I*) of 10 mA in the temperature range between 5 and 320 K and in magnetic fields between 0 and 40 kOe. These experiments were carried out using a Lake Shore model 7225 magnetometer. The external magnetic fields and excitation electrical currents were applied parallel and antiparallel to each other for all the measurements, i.e., only longitudinal magnetoresistance is considered in the present study. After slowly cooling the samples in zero magnetic field, the temperature dependencies of the electrical resistance, $R(T)$, were first measured during heating at a rate of 1 K/min from 5 to 320 K and then upon cooling at a similar rate. Every isothermal $R(H)$ measurement was recorded after thermal demagnetization by heating to 230 K and then slow cooling down to the measurement temperature in a zero magnetic field to exclude the magnetic field history dependence of the studied property.

The misorientation between the directions of the magnetic field vector and the crystal axes was less than $\pm 5^\circ$, considering the combined accuracy of crystallographic alignment and sample positioning inside the cryostat. The errors of the calculated electrical resistivity, $\rho = \frac{A}{l}R$, were about 10%, mainly due to the uncertainty in the measurement of the distance between voltage contacts, *l*, and the cross-sectional area of the sample, *A*. The magnetoresistance was calculated as $\text{MR} = \frac{\rho(H,T) - \rho(0,T)}{\rho(0,T)}$, where $\rho(H,T)$ and $\rho(0,T)$ represent the electrical resistivities at temperature, *T*, with and without the applied magnetic field, *H*, respectively. The electrical resis-

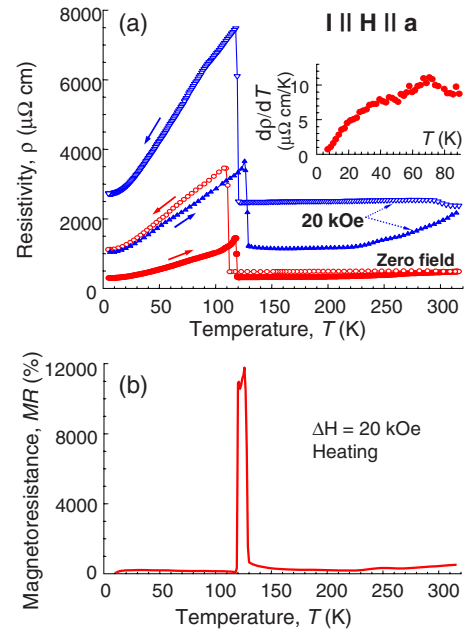


FIG. 1. (Color online) (a) Temperature (*T*) dependencies of the electrical resistivity (ρ) of the $\text{Tb}_5\text{Si}_{2.2}\text{Ge}_{1.8}$ single crystal measured upon heating (solid symbols) and cooling (open symbols) between 5 and 320 K in zero (circles) and 20 kOe (triangles) magnetic fields (*H*). Both *H* and 10 mA electrical current (*I*) were applied along the *a* axis of the crystal. The inset displays the first derivative of the electrical resistivity with respect to temperature, dp/dT , measured upon heating the sample in zero magnetic field. The arrows indicate the directions of the temperature variation. (b) Temperature dependence of the magnetoresistance calculated from the data in (a) without correcting for a stress build-up effect.

tivities at 5 K were subtracted to avoid the overestimation of the MR ratio due to a continuous increase in the electrical resistivity from extrinsic factors, such as accumulation of stress.

III. RESULTS AND DISCUSSION

A. Temperature dependencies of the electrical resistivity and magnetoresistance

The temperature dependencies of the electrical resistivity upon heating and cooling between 5 and 320 K in zero and 20 kOe magnetic fields applied along the *a* axis of $\text{Tb}_5\text{Si}_{2.2}\text{Ge}_{1.8}$ are shown in Fig. 1(a). The value of the electrical resistivity at 5 K in zero magnetic field (the first data point of the measurements) is about 300 $\mu\Omega$ cm and is of the same order as those observed in $\text{Tb}_5\text{Si}_2\text{Ge}_2$ and $\text{Tb}_5\text{Si}_{2.4}\text{Ge}_{1.6}$ polycrystalline samples.^{15,17} A local maximum is observed in the first derivative of the electrical resistivity with respect to temperature, dp/dT , at about 70 K, as shown in the inset of Fig. 1(a), corresponding to a spin-reorientation transition.^{18,21,26} Neither thermal nor magnetic field hysteresis is observed in the vicinity of this anomaly, therefore, only one curve (measured upon heating in zero magnetic field) is shown for clarity. The most distinct features in Fig. 1(a) are discontinuous changes in the electrical resistivity at various temperatures between 117 and 129 ± 1 K depending

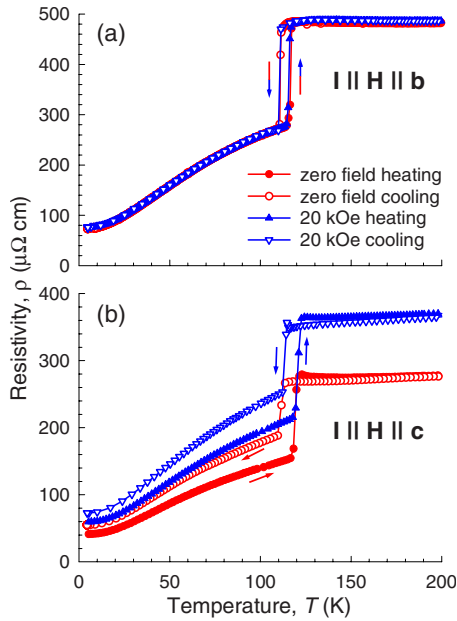


FIG. 2. (Color online) Temperature (T) dependencies of the electrical resistivity (ρ) of the $\text{Tb}_5\text{Si}_{2.2}\text{Ge}_{1.8}$ single crystal measured upon heating (solid symbols) and cooling (open symbols) between 5 and 200 K in zero (circles) and 20 kOe (triangles) magnetic fields (H). Both H and 10 mA electrical current (I) were applied along the b [(a)] and c [(b)] axes of the crystal. The arrows indicate the directions of the temperature variation.

on the direction of the temperature variation, i.e., heating or cooling, and the value of the applied magnetic field. Consistent with a first-order phase transformation between the low-temperature orthorhombic and high-temperature monoclinic structures,^{18,21,26} an 8 ± 1 K thermal hysteresis between the heating and cooling discontinuities is seen both with and without the applied magnetic field.

Figure 1(a) also shows that 20 kOe magnetic field applied along the a axis of $\text{Tb}_5\text{Si}_{2.2}\text{Ge}_{1.8}$ shifts the first-order phase transformation by 8 ± 1 K higher than that under zero magnetic field, i.e., $dT_C/dH = 0.4$ K/kOe. This together with the large change in the electrical resistivity during the phase transformation, results in an enormous value of magnetoresistance computed in the vicinity of the phase transformation, as shown in Fig. 1(b). In $\text{Tb}_5\text{Si}_{2.2}\text{Ge}_{1.8}$, 10 kOe and greater magnetic fields applied along its a -axis trigger simultaneously a magnetic order-disorder and a crystallographic order-order phase transformation,¹⁸ and therefore, the CMR effect here is related to the coupling of the magnetic and crystal lattices.

The temperature dependencies of the electrical resistivity along the b and c axes of $\text{Tb}_5\text{Si}_{2.2}\text{Ge}_{1.8}$ between 5 and 200 K are shown in Fig. 2. A comparison of the data shown in Figs. 1(a) and 2 demonstrates four major differences of the $\rho(T)$ along the three major crystallographic directions. First, the electrical resistivities along the b and c axes decrease as $\text{Tb}_5\text{Si}_{2.2}\text{Ge}_{1.8}$ transforms at T_C upon cooling, distinctly different from the increase observed along the a axis. Second, the virgin curves of the temperature dependencies of the electrical resistivity show a much greater electrical resistivity along the a axis compared to the same along the b and c axes; e.g.,

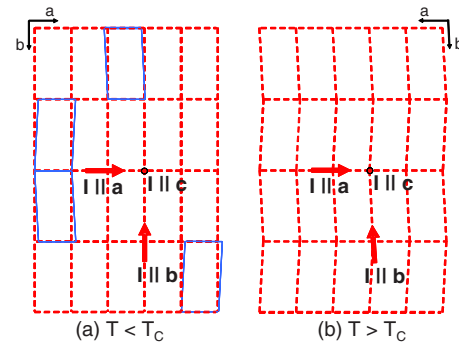


FIG. 3. (Color online) Two-dimensional schematic of the ab planes of the orthorhombic (a) and monoclinic (b) phases of $\text{Tb}_5\text{Si}_{2.2}\text{Ge}_{1.8}$. The dashed lines delineate the domains of the major phases in each case. The c axis is normal to the plane of the figure and is marked as a solid dot. The coherent length scale of domains is generally less than 10 nm (Ref. 27) and they are shown in identical sizes only for simplicity. The solid lines in (a) indicate the domains of the minor monoclinic phase retained in the long-lived phase-separated state.

at 5 K they are 300, 75, and 42 $\mu\Omega$ cm for the a , b , and c axes, respectively. Third, the change in the residual resistivity along the b axis upon cycling through T_C is nearly negligible and is the smallest compared to the other two axes of $\text{Tb}_5\text{Si}_{2.2}\text{Ge}_{1.8}$. Fourth, a 20 kOe magnetic field applied along the b and c axes does not change the first-order phase-transformation temperature thus leading to negligible magnetoresistance along the b axis and small magnetoresistance along the c axis.

These differences and the observed CMR effect along the a axis can be understood by recalling intrinsic crystallographic phase coexistence in $\text{Tb}_5\text{Si}_{2.2}\text{Ge}_{1.8}$. From an *in situ* x-ray diffraction study,¹⁸ the major orthorhombic (80 vol %) and the minor monoclinic (20 vol %) phases coexist in the ferromagnetically ordered state at a nearly constant volume fraction; while in the paramagnetic state, the sample is always a pure monoclinic phase. We note that the monoclinic structure is a distortion of the orthorhombic structure occurring via cooperative shear displacements of the adjacent atomic layers along the a axis.¹⁸ Considering the nanoscale twin structure of the monoclinic phase (5–10 nm),²⁷ the incoherent interphase boundaries between adjacent orthorhombic and monoclinic domains are located in the bc planes, as illustrated schematically in Fig. 3. Consequently, only the carriers moving along the a axis encounter additional scattering on large area with stress and disorder due to the mismatch at the interphase boundaries. Carriers moving along the b and c axes, on the contrary, are not affected much by these incoherent boundaries.

The movements of the layers of atoms that lie in the ac plane during the phase transformation and associated phase volume changes also quickly build-up internal stress, being most pronounced at the incoherent interphase boundaries but much less so along the b axis. Thus, continuous increases in the residual resistivities along the a and c axes with cycling are due to stress build up, and not due to the creation of microcracks. This conclusion was confirmed by remeasuring the cycled a -axis sample after it had been held at room tem-

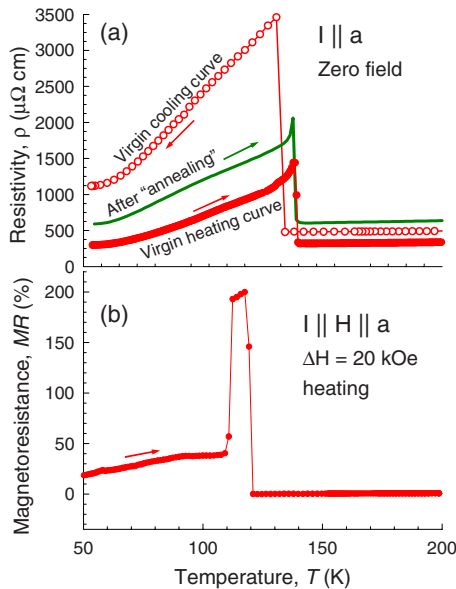


FIG. 4. (Color online) (a) A comparison of the temperature (T) dependencies of the electrical resistivity (ρ) of $\text{Tb}_5\text{Si}_{2.2}\text{Ge}_{1.8}$ between the virgin heating and cooling curves and initial heating curve after room-temperature “annealing.” The virgin curves are the same as the zero-field curves shown in Fig. 1(a). The after annealing curve was measured after the sample was cycled through the first-order phase transformation for 30 times and then “annealed” at room temperature for 21 months. Note: the virgin cooling curve represents the third run through the transition after the initial cooling to 5 K and the subsequent measurement on heating. The result after annealing is the second run through the transition after the initial cool down. (b) Temperature dependence of the magnetoresistance calculated from the data in Fig. 1(a) after subtracting the stress build-up effect. The arrows indicate the directions of the temperature variation.

perature for 21 months. After a 21-month room-temperature “anneal,” the zero-field resistivity drops substantially, nearly recovering the original residual resistance. A comparison of the two sets of data is shown in Fig. 4(a).

To eliminate the stress build-up effect on the computed magnetoresistance shown in Fig. 1(b), $\rho(0, T)$ was normalized by adding the difference between the zero and 20 kOe fields resistivities at 5 K and at the temperature right before the paramagnetic to ferromagnetic transition, for temperatures below and above the phase transition, respectively. Because the stress is partially self-annealed during the cooling process, the resistivity difference at 5 K is an underestimate of the effect over the whole ferromagnetic temperature range. This underestimation results in an artificial magnetoresistance in the ferromagnetic state along the a axis shown in Fig. 4(b). When this artificial contribution is subtracted from the peak magnetoresistance, a true peak magnetoresistance value becomes close to 160%, which is the same as that obtained in a direct measurement, as shown in Fig. 5(b), and discussed below.

B. Isothermal magnetic field dependence of magnetoresistance

The isothermal electrical-resistivity measurements as a function of magnetic field between zero and 40 kOe applied

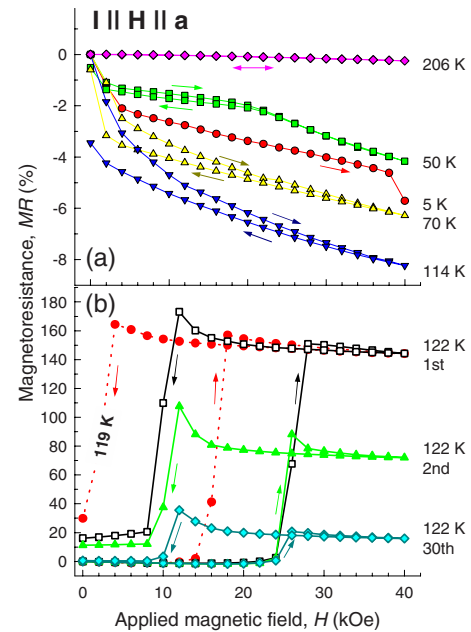


FIG. 5. (Color online) Isothermal magnetic field dependencies of magnetoresistance at selected temperatures measured with the magnetic field and electrical current applied along the a axis of $\text{Tb}_5\text{Si}_{2.2}\text{Ge}_{1.8}$. The arrows mark the direction of the magnetic field change. (a) shows the magnetoresistance below and well above the zero field $T_C=117$ K. (b) shows the magnetoresistance just above T_C .

along the a axis were carried out at selected temperatures. The resultant magnetoresistances are shown in Fig. 5. At temperatures just below and well above the first-order phase-transformation temperature, 117 K [taken as the temperature at the peak of the $\rho(T)$ curve upon heating in the zero magnetic field], the magnetoresistance exhibits typical behaviors of a ferromagnet and paramagnet, respectively, as seen in Fig. 5(a). The small negative values of the magnetoresistance manifest the reduction in the electron-magnon scattering by the external magnetic field. The hystereses between the field increasing and decreasing processes at and below 114 K can be assigned to the magnetic domain effect.

Notably, the 5 and 50 K curves show changes in their curvatures at 38 and 20 kOe, respectively, which coincide with the second-order spin reorientations observed in the dc magnetization data.²¹ In these transitions, the magnitudes of the magnetoresistance and magnetization both increase upon increasing external magnetic fields through these points, indicating the magnetic origin of these magnetoresistance anomalies. That is, the alignment of the canted magnetic moments by external magnetic field leads to further suppression of the electron-magnon scattering.

The magnitude of magnetoresistance decreases from 5 to 50 K, which can be explained by the increase in the zero magnetic field resistivity upon increasing temperature in a metal. According to Kohler’s rule,²⁸ $\text{MR} = \frac{\rho_H - \rho_0}{\rho_0} = f\left(\frac{H}{\rho_0}\right)$, the magnetoresistance is a function of the ratio ρ_H/ρ_0 (where ρ_H and ρ_0 are electrical resistivities under the applied magnetic field H and zero magnetic field, respectively, and f is a function determined by the electronic structure of the material).

An increase in ρ_0 causes a decrease in MR. Similar effect was also reported in another rare-earth intermetallic compound, LaAgSb₂.²⁹

The magnitude of the magnetoresistance of Tb₅Si_{2.2}Ge_{1.8} along the a axis, however, increases from 70 to 114 K. This can be understood considering that external magnetic fields are usually much more effective in the alignment of magnetic moments in a ferromagnet near its Curie point due to the weakening of the molecular-field effects by the thermal agitation thus giving rise to a strong reduction in the electron-magnon scattering over this temperature range, which is also the case in the rare-earth metal Gd.³⁰

Starting from 119 K, the magnetoresistance along the a axis of Tb₅Si_{2.2}Ge_{1.8} reaches 160% upon a first-order phase transformation, as seen in Fig. 5(b). The critical magnetic fields where the magnetoresistances start rising and dropping rapidly coincide with those of the first-order magnetic phase transition between the paramagnetic and ferromagnetic phases at the same temperatures,¹⁸ indicating the same origin of the abrupt changes in the magnetic states and electrical resistivities. The isothermal magnetization data (see Fig. 1 of Ref. 18) with the applied magnetic field along the a axis of Tb₅Si_{2.2}Ge_{1.8} between 119 and 130 K showed that increasing external magnetic field leads to a first-order transition from a paramagnetic to a ferromagnetic state. Normally, this results in a decrease in the electrical resistivity due to suppression of the electron-magnon scattering contribution. Therefore, the observed drastic increase in the electrical resistivity in Tb₅Si_{2.2}Ge_{1.8} along its a axis upon increasing the external magnetic field should be assigned to the magnetic field induced crystallographic phase transformation. Hence, direct measurements of the positive colossal magnetoresistance along the a axis are consistent with the model depicted in Fig. 3 (also see relevant discussion above).

It is well known that phase-coexistence states generally result from complicated energy landscapes and metastability is commonly observed in such systems manifesting itself as temperature or magnetic field history dependencies of physical properties. Thus, we conducted cycling experiments of the magnetic field dependence of the magnetoresistance of the Tb₅Si_{2.2}Ge_{1.8} along the a axis. Selected results of these measurements carried out at 122 K are shown in Fig. 5(b).

With cycling, the values of the magnetoresistances drop from 160% to \sim 90% from the first to the second cycle and then continue to fall reaching \sim 20% during the 30th cycle; meanwhile the sign of the magnetoresistances remain positive. The always positive magnetoresistance indicates that the coupling of the magnetically ordered state and the crystallographic phase coexistence persists during isothermal cycling. The large decrease in the magnitude of the magnetoresistance upon cycling can be directly related to a substantial increase in the zero-field resistivity at 122 K from 954.4 $\mu\Omega$ cm at the first cycle to 7782.4 $\mu\Omega$ cm at the 30th cycle. This increase in ρ (0 kOe, 122 K) can be attributed to two effects. First, the magnetic field induced crystallographic phase transformation is partially irreversible, i.e., the amount of the magnetic field induced orthorhombic phase continues to increase with cycling, which is evident from the *in situ* x-ray powder-diffraction study of the Tb₅Si_{2.2}Ge_{1.8} compound as shown in Fig. 6.³¹ Consequently, the number

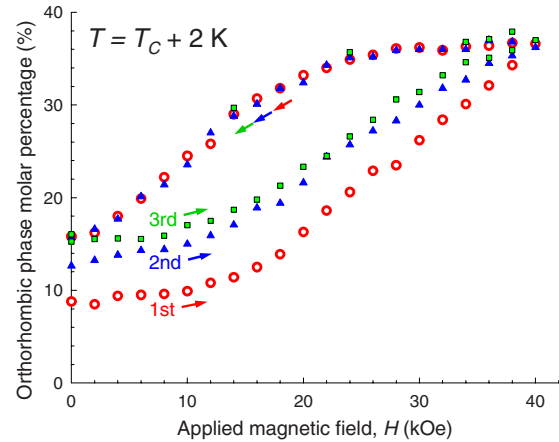


FIG. 6. (Color online) Isothermal magnetic field dependencies of the concentration of the orthorhombic phase of Tb₅Si_{2.2}Ge_{1.8} at 2 K above its Curie temperature (T_C). The concentration was determined from the Rietveld refinement of the x-ray powder-diffraction patterns recorded upon increasing and decreasing the applied magnetic field. The first set of data (open circles) was measured after thermal demagnetization by heating the sample to 230 K and then cooling down to the temperature 2 K above T_C without going below T_C . The second (solid triangles) and third (solid squares) sets of data were then measured successively. The arrows indicate the directions of the magnetic field change.

and area of the incoherent phase boundaries rise, leading to the observed increase in the zero magnetic field electrical resistivity. The second reason is the continuing stress build up as has been discussed above.

The longitudinal magnetoresistances of Tb₅Si_{2.2}Ge_{1.8} along the b axis are shown in Fig. 7(a). The positive magnetoresistances at 5 and 40 K are in line with the antiparallel configuration of the b -axis projection of the magnetic moments of Tb₅Si_{2.2}Ge_{1.8} at this temperature range. A simultaneous decrease and increase in the spin fluctuations of the moments parallel and antiparallel to the applied magnetic field, respectively, leads to a net increase in the electrical resistivity upon the increase in the external magnetic field, which was established both experimentally and theoretically for antiferromagnetic metals.^{32,33}

The magnetic field dependence of the magnetoresistance in Tb₅Si_{2.2}Ge_{1.8} along the b axis does not show a conventional $MR \propto H^2$ relationship as in a normal antiferromagnetic metal. This is understandable considering the complex non-collinear magnetic structure of the compound. The magnitudes of the magnetoresistances decrease with increasing temperature up to the ordering temperature, which is due to the increased zero magnetic field electrical resistance because the elevated temperature enhances both the electron-phonon and electron-magnon scatterings.

Interestingly, the magnetoresistance becomes negative at temperatures above 68 K even though the b -axis projections of the magnetic moments remain antiparallel to each other.²⁶ The change in the sign of the magnetoresistance is, therefore, related to the temperature-induced second-order magnetic-structure phase transition that occurs at 68 K.^{18,21,26} Above

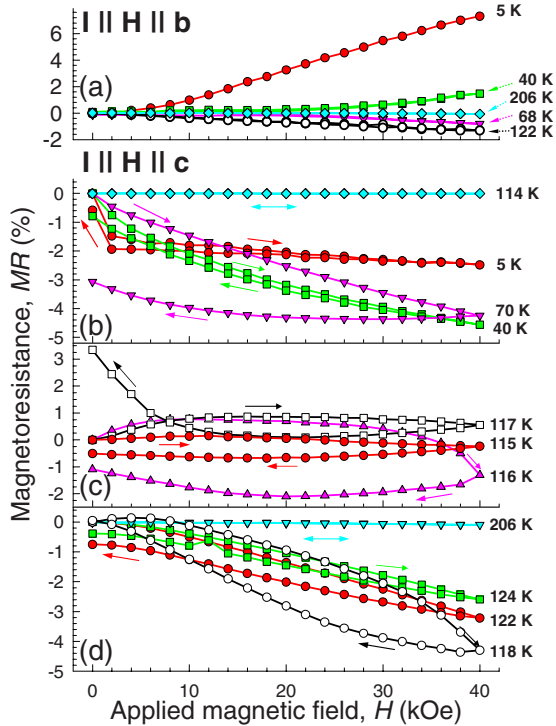


FIG. 7. (Color online) Isothermal magnetic field dependencies of magnetoresistance at selected temperatures measured with the applied magnetic field and electrical current (I) along the b [(a)] and c [(b)–(d)] axes of $\text{Tb}_5\text{Si}_{2.2}\text{Ge}_{1.8}$. The magnetizing curves start from the zero points. The arrows indicate the directions of the magnetic field change.

the first-order phase-transition temperature, the longitudinal magnetoresistance along the b axis is negative and decreases with increasing temperature, which is normal for the paramagnetic state of the compound. We note that there is almost no hysteresis of the longitudinal magnetoresistance along the b axis between the magnetic field increase and decrease processes.

Figures 7(b)–7(d) show the longitudinal magnetoresistances with the magnetic field applied along the c axis of $\text{Tb}_5\text{Si}_{2.2}\text{Ge}_{1.8}$. The magnetoresistances are negative between 5 and 70 K, see Fig. 7(b). A near saturation behavior is observed at 5 K, typical for a ferromagnet and in agreement with the observation of the c -axis projections of the magnetic moments of individual atoms being parallel at this temperature.²⁶ Interestingly, the magnetoresistance increases with increasing temperature from 5 to 40 K and then decreases from 40 to 114 K. Field hystereses were observed between 5 and 70 K with a maximum hysteresis at 70 K.

The magnetoresistance show several anomalies [Fig. 7(c)] near the zero-field first-order phase-transformation temperature, 117 K. During magnetizing, the magnetoresistance is positive between 115 and 117 K. During demagnetizing, the magnetoresistance is positive for 117 K but negative for 115 and 116 K and magnetoresistances at 118 K and higher temperatures exhibit behavior typical of a ferromagnet [see Fig. 7(d)], which may be evidence of the decoupling of the magnetic and crystallographic phase transitions, or of the appearance of a Griffiths-type phase in this compound.²¹

In addition to doped manganites, large magnetoresistance effects have been reported in pyrochlore $\text{Tl}_2\text{Mn}_2\text{O}_7$, Cr-based chalcogenide spinels, Eu-based hexaboride, doped silver chalcogenides, naturally layered LaMn_2Ge_2 , semimetallic Bi nanowire arrays, semiconducting InN film, GaAs/(AlGa)As, and Co-doped FeSb_2 .^{34–42} Magnetic field induced changes in spin-dependent scattering, manifested as a negative CMR,^{32–34} i.e., a decrease in the electrical resistivity when subjected to an applied magnetic field, is the underlying mechanism in all of these cases. This alone indicates a different mechanism from that observed in $\text{Tb}_5\text{Si}_{2.2}\text{Ge}_{1.8}$. For materials exhibiting positive CMR effect,^{38–42} the underpinning mechanisms were believed to be quantum interference effects, band splitting effects, or they were left without a feasible explanation. Yet, in the case of $\text{Tb}_5\text{Si}_{2.2}\text{Ge}_{1.8}$ it is the long-lived crystallographic phase coexistence that is responsible for the positive CMR effect.

IV. CONCLUSIONS

The electrical resistivities of $\text{Tb}_5\text{Si}_{2.2}\text{Ge}_{1.8}$ along its a , b , and c axes have been examined as functions of temperature and magnetic field. The electrical resistivity along the a axis is increased below the magnetic and crystallographic phase-transformation temperature but along the b and c axes the electrical resistivities show the opposite behavior, i.e., the resistivity is smaller in the magnetically ordered state. Positive colossal magnetoresistance with a magnitude of 160% is observed with the magnetic field applied along the a axis near the phase transformation. The magnetoresistance is conventional with the field applied along the b and c axes. The CMR effect originates from intrinsic crystallographic phase coexistence and long-lived phase-separated state. The scattering by the interphase boundaries in the bc plane leads to the anisotropy of the electrical resistivity and magnetoresistance.

The anisotropic magnetoresistance of $\text{Tb}_5\text{Si}_{2.2}\text{Ge}_{1.8}$ reveals a previously unknown control variable, which is the angle α between the CMR axis (here, the a axis of the crystal) and the magnetic field vector. By varying α between 0 and 90°, the magnetoresistance values may be tuned anywhere between 160% and ~ 0 . The change may be analogous to either switching a bit from 1 ($\alpha=0^\circ$) to 0 ($\alpha=90^\circ$) or to a variable resistor ($0 < \alpha < 90^\circ$). Further clarifications of such a distinct, yet relatively simple mechanism of the CMR at the nanoscale may open up new avenues for discovery of functional materials and for future applications in a variety of electronic devices. Both the magnetostructural phase transformation and the stable phase separation in the title and some other $R_5(\text{Si}_x\text{Ge}_{1-x})_4$ compounds can be triggered by variations in temperature and pressure⁴³ in addition to magnetic field. Hence, the phenomenology described above may also form a foundation for the design of multifunctional sensors that can simultaneously or separately detect changes in physically different stimuli.

ACKNOWLEDGMENTS

The Ames Laboratory is operated for the U.S. Department of Energy by Iowa State University under Contract No. DE-

AC02-07CH11358. This work was supported by the Office of Basic Energy Sciences, Materials Sciences Division of the U.S. Department of Energy.

*Corresponding author; zoumin@iastate.edu

- ¹A. Barthelemy, A. Fert, and F. Petroff, in *Handbook of Magnetic Materials*, edited by K. Buschow (Elsevier, North-Holland, Amsterdam, 1999), Vol. 12, p. 1.
- ²A. P. Ramirez, *J. Phys.: Condens. Matter* **9**, 8171 (1997).
- ³C. N. R. Rao and A. K. Raychaudhuri, in *Colossal Magnetoresistance, Charge Ordering and Related Properties of Manganese Oxides*, edited by C. N. R. Rao and B. Raveau (World Scientific, Singapore, 1998), p. 1.
- ⁴J. M. D. Coey, M. Viret, and S. von Molnar, *Adv. Phys.* **48**, 167 (1999).
- ⁵Y. Tokura and Y. Tomioka, *J. Magn. Magn. Mater.* **200**, 1 (1999).
- ⁶C. N. R. Rao, A. Arulraj, A. K. Cheetham, and B. Raveau, *J. Phys.: Condens. Matter* **12**, R83 (2000).
- ⁷L. Morellon, J. Stankiewicz, B. Garcia-Landa, P. A. Algarabel, and M. R. Ibarra, *Appl. Phys. Lett.* **73**, 3462 (1998).
- ⁸E. M. Levin, V. K. Pecharsky, and K. A. Gschneidner, Jr., *Phys. Rev. B* **60**, 7993 (1999).
- ⁹L. Morellon, P. A. Algarabel, C. Magen, and M. R. Ibarra, *J. Magn. Magn. Mater.* **237**, 119 (2001).
- ¹⁰H. Tang, V. K. Pecharsky, G. D. Samolyuk, M. Zou, K. A. Gschneidner, Jr., V. P. Antropov, D. L. Schlagel, and T. A. Lograsso, *Phys. Rev. Lett.* **93**, 237203 (2004).
- ¹¹E. M. Levin, V. K. Pecharsky, K. A. Gschneidner, Jr., and P. Tomlinson, *J. Magn. Magn. Mater.* **210**, 181 (2000).
- ¹²E. M. Levin, A. O. Pecharsky, V. K. Pecharsky, and K. A. Gschneidner, Jr., *Phys. Rev. B* **63**, 064426 (2001).
- ¹³V. K. Pecharsky and K. A. Gschneidner, Jr., *Adv. Mater. (Weinheim, Ger.)* **13**, 683 (2001).
- ¹⁴C. Ritter, L. Morellon, P. A. Algarabel, C. Magen, and M. R. Ibarra, *Phys. Rev. B* **65**, 094405 (2002).
- ¹⁵L. Morellon, C. Ritter, C. Magen, P. A. Algarabel, and M. R. Ibarra, *Phys. Rev. B* **68**, 024417 (2003).
- ¹⁶J. P. Araújo, A. M. Pereira, M. E. Braga, R. P. Pinto, J. M. Teixeira, F. C. Correia, J. B. Sousa, L. Morellon, P. A. Algarabel, C. Magen, and M. R. Ibarra, *J. Phys.: Condens. Matter* **17**, 4941 (2005).
- ¹⁷Y. D. Yao, S. F. Lee, M. D. Lee, K. T. Wu, D. G. Cheng, N. P. Thuy, N. T. Hien, L. T. Tai, T. Q. Vinh, and N. V. Nong, *Physica B (Amsterdam)* **327**, 324 (2003).
- ¹⁸M. Zou, Ya. Mudryk, V. K. Pecharsky, K. A. Gschneidner, Jr., D. L. Schlagel, and T. A. Lograsso, *Phys. Rev. B* **75**, 024418 (2007).
- ¹⁹R. Nirmala, Ya. Mudryk, V. K. Pecharsky, and K. A. Gschneidner, Jr., *Phys. Rev. B* **76**, 104417 (2007).
- ²⁰C. Magen, P. A. Algarabel, L. Morellon, J. P. Araújo, C. Ritter, M. R. Ibarra, and J. B. Sousa, *Phys. Rev. Lett.* **96**, 167201 (2006).
- ²¹M. Zou, V. K. Pecharsky, K. A. Gschneidner, Jr., D. L. Schlagel, and T. A. Lograsso, *Phys. Rev. B* **78**, 014435 (2008).
- ²²M. B. Salamon, P. Lin, and S. H. Chun, *Phys. Rev. Lett.* **88**, 197203 (2002).
- ²³J. Burgy, M. Mayr, V. Martin-Mayor, A. Moreo, and E. Dagotto, *Phys. Rev. Lett.* **87**, 277202 (2001).
- ²⁴D. L. Schlagel, T. A. Lograsso, A. O. Pecharsky, and J. A. Sampaio, in *Light Metals 2005*, edited by H. Kvande (The Minerals, Metals and Materials Society, TMS, Warrendale, PA, 2005), p. 1177.
- ²⁵Materials Preparation Center, The Ames Laboratory, US Department of Energy, Ames, IA, USA, www.mpc.ameslab.gov
- ²⁶V. O. Garlea, J. L. Zarestky, C. Y. Jones, L.-L. Lin, D. L. Schlagel, T. A. Lograsso, A. O. Tsokol, V. K. Pecharsky, K. A. Gschneidner, Jr., and C. Stassis, *Phys. Rev. B* **72**, 104431 (2005).
- ²⁷Z. W. Du, A. S. Liu, B. L. Shao, Z. Y. Zhang, X. S. Zhang, and Z. M. Sun, *Mater. Charact.* **59**, 1241 (2008).
- ²⁸A. B. Pippard, *Magnetoresistance in Metals* (Cambridge University Press, Cambridge, 1989).
- ²⁹K. D. Myers, Ph.D. thesis, Iowa State University, 1999.
- ³⁰P. P. Freitas and J. B. Sousa, *J. Phys. F: Met. Phys.* **13**, 1245 (1983).
- ³¹The data in Fig. 6 were collected using the same *in situ* x-ray powder-diffraction sample and experiment methods and instruments as in Ref. 18.
- ³²H. Yamada and S. Takada, *Prog. Theor. Phys.* **52**, 1077 (1974).
- ³³H. Nagasawa, *Phys. Lett. A* **41**, 39 (1972).
- ³⁴Y. Shimakawa, Y. Kubo, and T. Manako, *Nature (London)* **379**, 53 (1996).
- ³⁵A. P. Ramirez, R. J. Cava, and J. Krajewski, *Nature (London)* **386**, 156 (1997).
- ³⁶G. A. Wigger, C. Beeli, E. Felder, H. R. Ott, A. D. Bianchi, and Z. Fisk, *Phys. Rev. Lett.* **93**, 147203 (2004).
- ³⁷R. Xu, A. Husmann, T. F. Rosenbaum, M.-L. Saboungi, J. E. Enderby, and P. B. Littlewood, *Nature (London)* **390**, 57 (1997).
- ³⁸R. Mallik, E. V. Sampathkumaran, and P. L. Paulose, *Appl. Phys. Lett.* **71**, 2385 (1997).
- ³⁹Kimin Hong, F. Y. Yang, Kai Liu, D. H. Reich, P. C. Searson, C. L. Chien, F. F. Balakirev, and G. S. Boebinger, *J. Appl. Phys.* **85**, 6184 (1999).
- ⁴⁰C.-T. Liang, Zhi-Hao Sun, Ching-Lien Hsiao, M. Z. Hsu, Li-Wei Tu, Jyun-Ying Lin, Jing-Han Chen, Y. F. Chen, and Chien Ting Wu, *Appl. Phys. Lett.* **90**, 172101 (2007).
- ⁴¹Chien-Chung Wang, C.-T. Liang, Yu-Ting Jiang, Y. F. Chen, N. R. Cooper, M. Y. Simmons, and D. A. Ritchie, *Appl. Phys. Lett.* **90**, 252106 (2007).
- ⁴²Rongwei Hu, V. F. Mitrović, and C. Petrovic, *Phys. Rev. B* **74**, 195130 (2006).
- ⁴³Ya. Mudryk, Y. Lee, T. Vogt, K. A. Gschneidner, Jr., and V. K. Pecharsky, *Phys. Rev. B* **71**, 174104 (2005).